

A comparison of untagged gamma-ray and tagged-neutron yields from $^{241}\text{AmBe}$ and $^{238}\text{PuBe}$ sources

J. Scherzinger^{a,b}, R. Al Jebali^c, J.R.M. Annand^c, K.G. Fissum^{a,b,*},
R. Hall-Wilton^{b,d}, S. Koufigar^{a,1}, N. Mauritzson^a, F. Messi^a, H. Perrey^{a,b},
E. Rofors^a

^a*Division of Nuclear Physics, Lund University, SE-221 00 Lund, Sweden*

^b*Detector Group, European Spallation Source ESS AB, SE-221 00 Lund, Sweden*

^c*SUPA School of Physics and Astronomy, University of Glasgow, Glasgow G12 8QQ, Scotland, UK*

^d*Mid-Sweden University, SE-851 70 Sundsvall, Sweden*

Abstract

Untagged gamma-ray and tagged-neutron yields from $^{241}\text{AmBe}$ and $^{238}\text{PuBe}$ mixed-field sources have been measured. Gamma-ray spectroscopy measurements from 1 – 5 MeV were performed in an open environment using a CeBr_3 detector and the same experimental conditions for both sources. The shapes of the distributions are very similar and agree well with previous data. Tagged-neutron measurements from 2 – 6 MeV were performed in a shielded environment using a NE-213 liquid-scintillator detector for the neutrons and a YAP(Ce) detector to tag the 4.44 MeV gamma-rays associated with the de-excitation of the first excited state of ^{12}C . Again, the same experimental conditions were used for both sources. The shapes of these distributions are also very similar and agree well with previous data, each other, and the ISO recommendations. Our $^{238}\text{PuBe}$ source provides approximately 2.4 times more tagged neutrons over the tagged-neutron energy range, in reasonable agreement with the original full-spectrum source-calibration measurements performed at the time of

*Corresponding author. Telephone: +46 46 222 9677; Fax: +46 46 222 4709

Email address: kevin.fissum@nuclear.lu.se (K.G. Fissum)

¹present address: Applied Physics and Applied Mathematics Department, Columbia University, New York, NY 10027, USA

their acquisition.

Keywords: americium-beryllium, plutonium-beryllium, gamma-rays, fast neutrons, time-of-flight, pulse-shape discrimination, NE-213, cerium-bromide

1. Introduction

Actinide/Be-based radioactive sources are typically used for cost-effective fast-neutron irradiations. Neutrons are produced when the α -particle from the decay of the actinide interacts with the ${}^9\text{Be}$ nucleus. If one is only interested in neutrons, a major drawback associated with these sources is the gamma-ray field produced by the original actinide. Higher-energy gamma-rays are also produced via the $\alpha + {}^9\text{Be} \rightarrow \text{n} + {}^{12}\text{C}^*$ reaction. However, if detected, these 4.44 MeV gamma-rays can be used to “tag” the corresponding neutrons [1], resulting in a polychromatic energy-tagged neutron beam. In this paper, we employ the neutron-tagging technique to measure tagged, fast-neutron yields from ${}^{241}\text{AmBe}$ and ${}^{238}\text{PuBe}$ using a NE-213 liquid-scintillator detector. We also measure the corresponding untagged gamma-ray yields using a Cerium-bromide (CeBr_3) detector. Our goal was to measure the tagged-neutron yields provided by the two sources and identify which of the two sources provided the higher tagged-neutron yield.

2. Apparatus

2.1. Actinide/Be-based sources

For the investigations performed in this work, both ${}^{241}\text{Am}/{}^9\text{Be}$ (Am/Be) and ${}^{238}\text{Pu}/{}^9\text{Be}$ (Pu/Be) sources were employed. Both actinides decay predominantly via the emission of α -particles. According to NuDat [2], ${}^{241}\text{Am}$ decays via the emission of 25 different α -particles (5.4786 MeV weighted-mean energy) while ${}^{238}\text{Pu}$ decays via the emission of 14 different α -particles (5.4891 MeV weighted-mean energy). The difference in the weighted mean α -particle energies is thus only about 10 keV. When these α -particles interact with ${}^9\text{Be}$, fast neutrons are produced. Because the weighted mean of the incident α -particle energies



Figure 1: The detectors employed for the measurements presented in this paper. From the left: NE-213 liquid-scintillator neutron and gamma-ray detector; CeBr_3 gamma-ray spectroscopy detector; YAP(Ce) gamma-ray trigger detector.

is essentially the same for both actinides, the energy spectra of emitted neutrons are anticipated to demonstrate strong similarities. These neutrons have a maximum energy of about about 11 MeV [3]. If the recoiling ^{12}C is left in its first excited state, the freed neutron is accompanied by an isotropically radiated prompt 4.44 MeV de-excitation gamma-ray. The radiation fields associated with these sources are thus a combination of the gamma-ray field associated with the original actinide together with 4.44 MeV gamma-rays and their associated fast-neutrons. Our Am/Be source radiates approximately 1.14×10^6 neutrons per second [4], while our Pu/Be source radiates approximately 2.99×10^6 neutrons per second [5], both nearly isotropically.

2.2. Detectors

The NE-213 liquid-scintillator and YAP(Ce) and CeBr_3 gamma-ray detectors used in the measurements used for this work are shown in Fig. 1.

2.2.1. NE-213 liquid-scintillator detector

NE-213 [6] is a standard organic liquid scintillator which has been employed for several decades for detecting neutrons in strong gamma-ray fields. Because gamma-ray induced scintillations in NE-213 are generally fast (10s of ns decay times) while neutron induced scintillations are much slower (100s of ns decay times), the type of radiation incident upon the NE-213 scintillator may be identified by examining the time structure of the scintillation pulses. The pseudocumene-based NE-213 liquid-scintillator detector employed in this measurement consisted of a 3 mm thick cylindrical aluminum cell (62 mm long \times 94 mm \varnothing) coated internally with EJ-520 TiO₂-based reflective paint [7] which contained the NE-213. A 5 mm thick borosilicate glass plate [8] was used as an optical window. The filled cell was coupled to a cylindrical PMMA UVT lightguide [9] (57 mm long \times 72.5 mm \varnothing) coated on the outside by EJ-510 [10] TiO₂-based reflective paint. The assembly was coupled to a μ -metal shielded 3 in. ET Enterprises 9821KB photomultiplier tube (PMT) and base [11]. Operating voltage was set at about -1900 V, and the energy calibration was determined using standard gamma-ray sources together with a slightly modified version of the method of Knox and Miller [12]. See Refs. [1, 13] for more detail.

2.2.2. YAP(Ce) 4.44 MeV gamma-ray detectors

The YAP(Ce) (YAlO₃, Ce⁺ doped) gamma-ray detectors employed in this measurement were provided by Scionix [14]. Each detector was comprised of a cylindrical (2.54 cm long \times 2.54 cm \varnothing) crystal [15] attached to 2.54 cm Hamamatsu Type R1924 PMT [16]. YAP(Ce) is a useful gamma-ray trigger scintillator in a strong radiation field as it is both radiation hard and relatively insensitive to fast neutrons. Operating voltage was set at about -800 V, and energy calibration was determined using standard gamma-ray sources. These YAP(Ce) detectors were used to count the 4.44 MeV gamma-rays emanating from the sources and thus tag the corresponding emitted neutrons. See Refs. [1, 13] for more detail.

2.2.3. *CeBr₃ gamma-ray detector*

The CeBr₃ gamma-ray detector employed in this measurement was provided by Scionix [14]. The detector was comprised of a cylindrical (3.81 cm long \times 3.81 cm \varnothing) crystal [17] attached to a 5.08 cm Hamamatsu Type R6231 PMT [16]. Due to its fast response without slow scintillation components and excellent energy resolution (3.8% FWHM for the full-energy peak produced by the 662 keV gamma-ray from ¹³⁷Cs), CeBr₃ is a useful scintillator for gamma-ray spectroscopy. Operating voltage was set at about -850 V, and energy calibration was determined using standard gamma-ray sources. The CeBr₃ gamma-ray detector was used to measure the gamma-ray spectra associated with the Am/Be and Pu/Be sources.

3. Measurement

3.1. Setup

The measurements described below were performed sequentially for each of the actinide/Be sources. The CeBr₃ detector used for gamma-ray spectroscopy was located 50 cm from the source and placed at source height. Neutron shielding by organic materials or water was not employed to avoid production of 2.23 MeV gamma-rays from neutron capture on protons. The threshold for the CeBr₃ detector was set at about 350 keV. For the neutron-tagging measurements, water and plastic shielding were employed to define a neutron beam. Four YAP(Ce) 4.44 MeV gamma-ray trigger detectors were individually positioned around the source at a distance of about 10 cm and placed slightly above the height of the source. The threshold for the YAP(Ce) detectors was also set at about 350 keV. The NE-213 detector was located 110 cm from the source and placed also at source height. The threshold for the NE-213 detector was set at about 200 keV_{ee} (keV electron equivalent). In the energy region above 1 MeV, all of the detectors triggered largely on the 4.44 MeV gamma-rays emanating from the source. The NE-213 detector triggered on both gamma-rays and neutrons produced by the source. Neutron time-of-flight (TOF) and thus energy

was determined by detecting both the fast neutron in the NE-213 detector and the prompt correlated 4.44 MeV gamma-ray in a YAP(Ce) detector. By tagging the neutrons in this fashion, the neutron yield as a function of kinetic energy was measured. Note that due to the energy lost to the 4.44 MeV gamma-ray, the tagging technique restricted the maximum available tagged-neutron energies to about 6 MeV.

3.2. Electronics and data acquisition

The analog signals from the NE-213 detector were sent to Phillips Scientific (PS) 715 NIM constant-fraction timing discriminators (CFDs) as well as LeCroy (LRS) 10-bit 2249A (DC-coupled 60 ns short gate SG) and 11-bit 2249W (AC-coupled 500 ns long gate LG) CAMAC charge-to-digital converters (QDCs). The analog signals from the CeBr₃ detector were sent to PS715 NIM CFDs as well as CAEN V792 12-bit (DC-coupled 60 ns gate) VME QDCs. For both the tagged-neutron and untagged gamma-ray measurements, the CFD signals were used to trigger the data-acquisition (DAQ). For the tagged-neutron measurements, the CFD signals from the NE-213 detector also provided start signals for LRS 2228A CAMAC time-to-digital converters (TDCs) used for the neutron TOF determination. The YAP(Ce) detector provided the corresponding (delayed) stop signal for this TOF TDC. A CES 8210 branch driver was employed to connect the CAMAC electronics to a VMEbus and a SIS 3100 PCI-VME bus adapter was used to connect the VMEbus to a LINUX PC-based DAQ system. The signals were recorded and processed using ROOT-based software [18]. See Refs. [1, 13] for more detail.

4. Results

4.1. Pulse-shape discrimination (PSD)

We employed the “tail-to-total” method [19–21] to analyze the time dependence of the scintillation pulses to discern between gamma-rays and neutrons. The pulse shape (PS) was defined as

$$PS = (LG - SG)/LG, \quad (1)$$

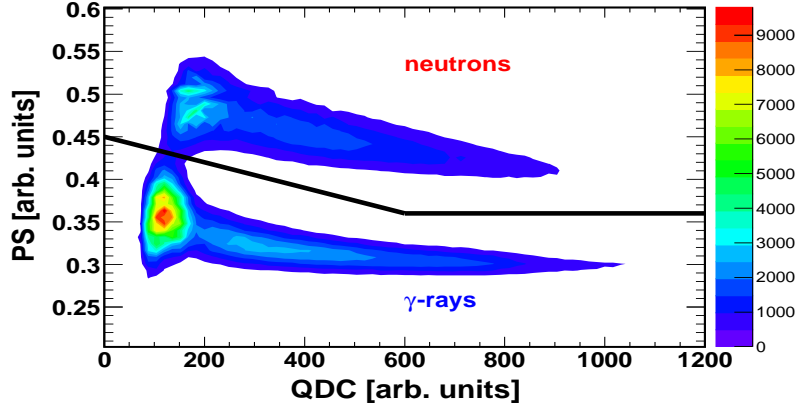


Figure 2: Typical PSD contour plot obtained using the actinide/Be sources. PS has been plotted against the total energy deposited in the LG QDC. The upper band corresponds to neutrons while the lower band corresponds to gamma-rays. The black line indicates the neutron cut applied to obtain subsequent spectra. (For interpretation of the references to color in this figure caption, the reader is referred to the web version of this article.)

where LG and SG were the integrated charges produced by the scintillation-light pulses in the LG and SG QDCs, respectively. Figure 2 shows a contour PSD distribution obtained using the Pu/Be source when the NE-213 detector started the TOF TDC and the YAP(Ce) detector stopped the TOF TDC. Separation between neutrons and gamma-rays was excellent.

4.2. Time-of-flight (TOF)

Data from the TOF TDC were calibrated and used to establish the neutron time-of-flight. Correlated gamma-ray pairs originating in the sources and detected one in the NE-213 detector and one in a YAP(Ce) detector provided a “gamma-flash”². T_0 , the instant of emission of the neutron from the source, was

²For example, from the α decay of ^{241}Am to an excited state of ^{237}Np .

determined from the location of the gamma-flash in the TOF spectra using the speed of light and measurements of the distances between the YAP(Ce) detector, the NE-213 detector, and the source. In the top panel of Fig. 3, the excellent separation between gamma-rays and neutrons is illustrated in a contour plot of PS against TOF. In the bottom panel, the contour plot has been projected onto the TOF axis. Further, the black-line cut from Fig. 2 has been applied, and a TOF distribution for events identified as neutrons is shown. The gamma-flash has a FWHM of about 1.5 ns (arising from the timing jitter in our signals) and is located at 3.5 ns. Tagged neutrons dominate the plot between 30 ns and 70 ns. Events between 8 and 30 ns and for TOF > 70 ns are mainly due to random coincidences. Random events included source-related gamma-rays and neutrons and depended on the singles rates in the YAP and NE-213 detectors.

4.3. Untagged gamma-ray yields

Figure 4 shows our untagged gamma-ray yields obtained with the CeBr₃ detector. Other than cycling the sources, no changes were made to the apparatus. A software cut has been placed at 1 MeV to exclude very low energy gamma-ray events, including room-associated background. Over this energy range, the gamma-ray field from the Pu/Be source is clearly stronger than that from the Am/Be source, but the structure is very similar. The structures in the Pu/Be and Am/Be gamma-ray distributions 3 and 5 MeV correspond to neutron-associated gamma-rays from the de-excitation of ¹²C*. The full-energy peak appears at 4.44 MeV, while the corresponding first- and second-escape peaks appear at 3.93 MeV and 3.42 MeV, respectively. The peak at 2.61 MeV corresponds to the de-excitation of ²⁰⁸Pb* to its ground state and is due to room background.

4.4. Tagged-neutron yields

Figure 5 shows our actinide/Be tagged-neutron results obtained by measuring the neutron TOF between the NE-213 trigger and YAP(Ce) 4.44 MeV gamma-ray detectors. Our data are livetime-corrected yields – they have not

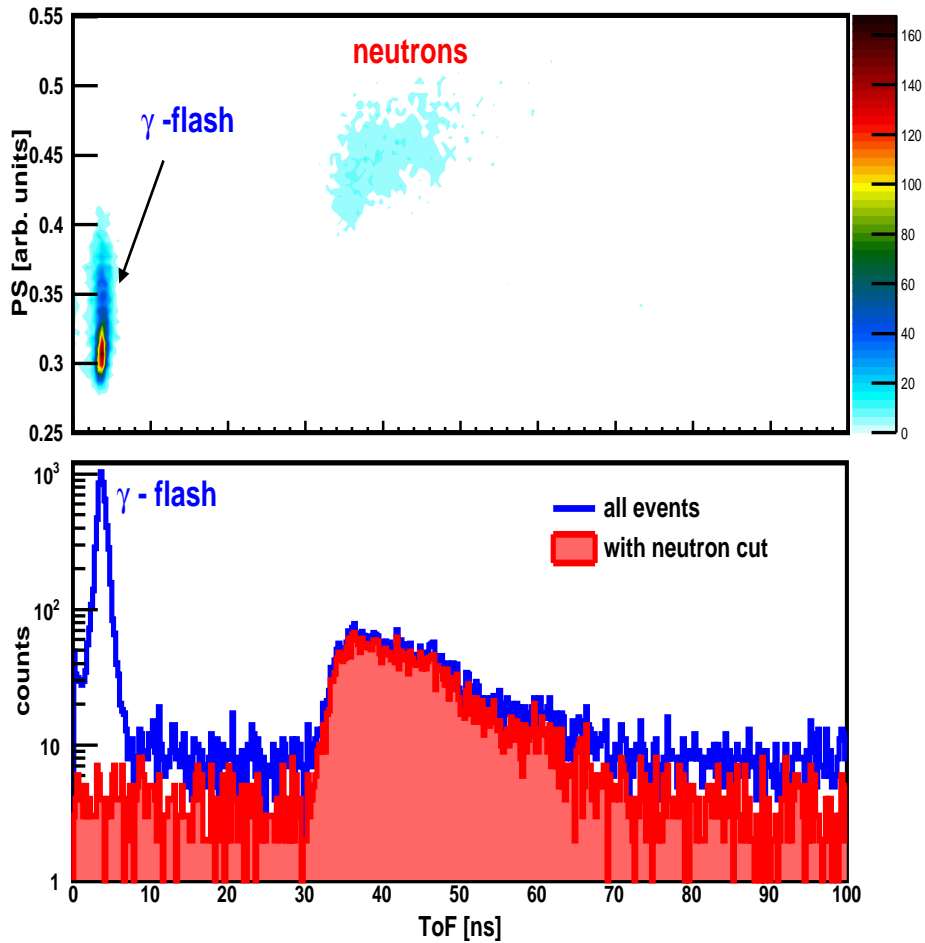


Figure 3: Typical TOF distributions obtained using the actinide/Be sources. In the top panel, PS has been plotted against TOF. Gamma-rays from the gamma-flash are shown to the left of the plot, while neutrons are shown in the center. In the bottom panel, TOF distributions have been plotted for all events (unshaded blue) as well as events identified as neutrons (shaded red). The peak in the unshaded blue distribution located at about 4 ns is the gamma-flash. (For interpretation of the references to color in this figure caption, the reader is referred to the web version of this article.)

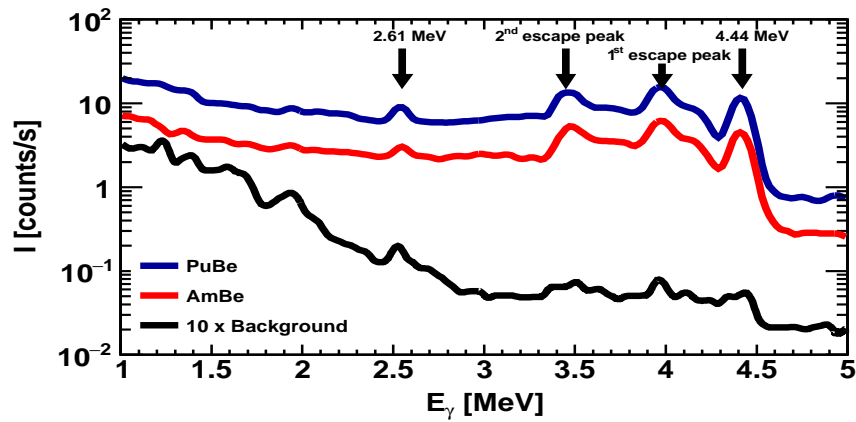


Figure 4: Untagged livetime-corrected gamma-ray yields. The dark blue distribution corresponds to the gamma-ray field measured from the Pu/Be source, the red distribution corresponds to the gamma-ray field measured from the Am/Be source, and the light-blue distribution corresponds to the gamma-ray field measured without a source. (For interpretation of the references to color in this figure caption, the reader is referred to the web version of this article.)

been corrected for neutron-detection efficiency or detector acceptance. Note that other than physically swapping the actinide/Be sources, absolutely no changes were made to our apparatus during data acquisition. In both panels, the maximum values of the Lorch spectra at ~ 3 MeV have been normalized to our distributions. Due to the neutron-tagging procedure, our data show no strength above ~ 7 MeV as 4.44 MeV is taken by the creation of the de-excitation gamma-ray. Our results for Am/Be presented in the top panel are shown together with the widely quoted full-energy neutron spectrum of Lorch [3]³ and the ISO 8529-2 reference neutron radiation spectrum. Agreement between the Lorch data and the reference spectrum is very good between 2.5 MeV and 10 MeV. Lorch did not observe the strength above 10 MeV present in the reference spectrum. The Lorch data display a sharp cutoff at 2.5 MeV which is attributed to an analysis threshold cut. The reference spectrum shows considerable strength below 2.5 MeV. Our data also show some strength in this region. Recall that our hardware threshold was 200 keV_{ee} corresponding to a neutron energy of ~ 1 MeV, and that no analysis threshold cut was employed. The agreement between our data, those of Lorch, and the reference spectrum in the region of overlap is excellent. The interested reader is directed to Ref. [1] for a detailed discussion. Our results for Pu/Be presented in the bottom panel are shown together with those of Kozlov et al. [22]. The Kozlov et al. measurement involved detecting the neutrons emitted from a series of “homemade” Pu/Be sources in a cylindrical (30 mm long \times 30 mm \varnothing) stilbene crystal. Statistical uncertainties in these results were reported to be better than 3% below 5 MeV and better than 20% at 10 MeV. Similar to the Lorch data discussed above, the Kozlov et al. data also display a sharp cutoff at 2.5 MeV. While it is not possible to determine

³ The results we present in this paper are for a newly acquired Am/Be source that is different from the source that we used to produce the results presented in Ref. [1]. Due to flight-path differences and the resulting resolution effects, it is difficult to exactly compare the two data sets. Nevertheless, over the energy range 2 – 6 MeV, the difference in the tagged-neutron yields (normalized at 3 MeV) obtained with the two different sources is less than 2%.

the reason for this cutoff from the information presented in Ref. [22], we again attribute it to an analysis threshold cut. Recall that our hardware threshold was 200 keV_{ee} corresponding to a neutron energy of ~ 1 MeV, and that no analysis threshold cut was employed. Agreement between the Kozlov et al. data and ours is very good between 2.5 MeV and 6 MeV. Finally, we note the qualitative agreement between our Am/Be and Pu/Be results, the Lorch and Kozlov et al. results, and the ISO ISO8529-2 reference neutron radiation spectrum.

Figure 6 presents a quantitative comparison between the livetime-corrected tagged-neutron yields for our Am/Be and Pu/Be sources. The (Pu/Be) : (Am/Be) ratio is taken from the gray-shaded regions presented in Fig. 5 and is displayed for the energy region over which we are confident that we are not simply seeing effects from applied hardware thresholds. The mean value of the ratio between 2 and 6 MeV is 2.4, which is in reasonable agreement with the original full-spectrum source-calibration measurements performed at the time of their acquisition. Explanation of the observed fluctuation in the ratio as a function of neutron energy requires a more detailed study of the possible effects of source composition, neutron-detection efficiency, and detector acceptances. This will be covered in future work.

5. Summary

We have measured untagged gamma-ray and tagged neutron yields from $^{241}\text{AmBe}$ and $^{238}\text{PuBe}$ sources. Our untagged gamma-ray distributions ranged from 1 – 5 MeV. They were performed in an open environment with the same experimental conditions for both sources. The shapes of the distributions are very similar and are clearly dominated by the 4.44 MeV gamma-ray associated with the de-excitation of the first excited state in ^{12}C . Our tagged-neutron distributions ranged from 2 – 6 MeV. They were performed in a shielded environment with the same experimental conditions for both sources. The shapes of the distributions are quite similar and agree well with previous data obtained for the respective sources. Further, the shape of the Am/Be distribution agrees well

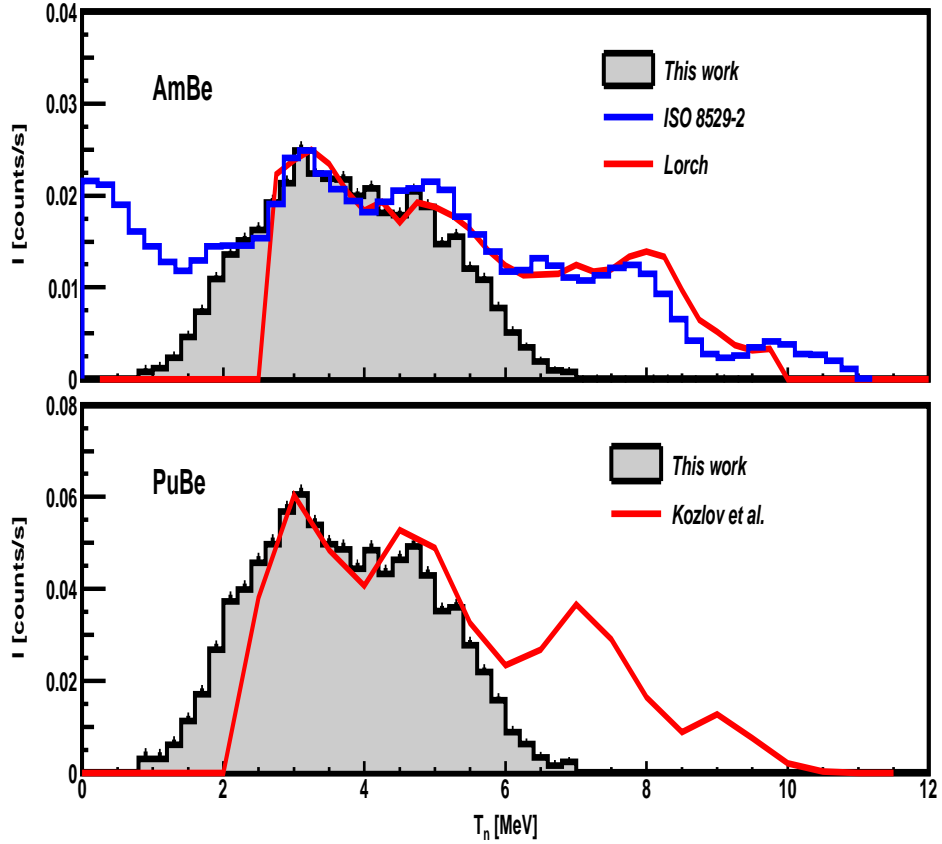


Figure 5: Tagged-neutron results. The gray-shaded histograms are our livetime-corrected tagged-neutron measurements. Note the different y-axis scales in the top and bottom panel. Top panel: Am/Be. The full-energy spectrum (red line) of Lorch [3] is also shown together with the Am/Be ISO 8529-2 reference neutron radiation spectrum. Bottom panel: Pu/Be. The full-energy spectrum (red line) of Kozlov et al. [22] is also shown. (For interpretation of the references to color in this figure caption, the reader is referred to the web version of this article.)

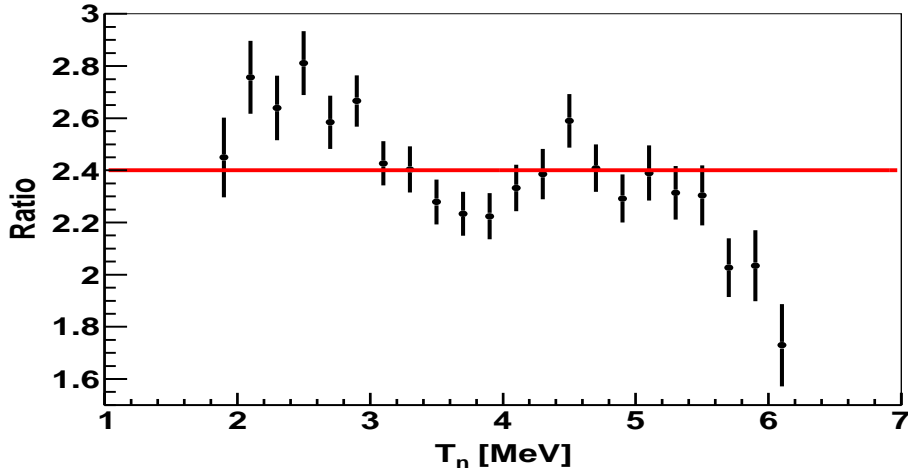


Figure 6: Livetime-corrected (Pu/Be) : (Am/Be) ratio of tagged-neutron yields.

with the ISO 8529-2 reference neutron radiation spectrum. We determined that our Pu/Be source emits roughly 2.4 times as many taggable neutrons as our Am/Be source, in reasonable agreement with the original full-spectrum source-calibration measurements performed at the time of their acquisition. Observed differences in the details of the shape of the neutron spectra will be the subject of future investigations.

Acknowledgements

We acknowledge the support of the UK Science and Technology Facilities Council (Grant nos. STFC 57071/1 and STFC 50727/1) and the European Union Horizon 2020 BrightnESS Project, Proposal ID 676548.

References

- [1] J. Scherzinger et al., *Applied Radiation and Isotopes* 98 (2015) 74, doi: 10.1016/j.apradiso.2015.01.003.
- [2] <http://www.nndc.bnl.gov/nudat2/>.
- [3] E.A. Lorch, *Int. J. Appl. Radiat. Is.* 24 (1973) 585, doi: 10.1016/0020-708X(73)90127-0.
- [4] Exactly $(1.143 \pm 0.015) \times 10^6$ neutrons per second. Testing certified at National Physical Laboratory, Teddington, Middlesex, UK TW11 0LW on 24 July 2015.
- [5] Exactly 4.26×10^6 neutrons per second. Calibration certified at The Radiochemical Centre, Amersham, England HP7 9LL on 3 September, 1973.
- [6] Eljen Technologies EJ-301 (<http://www.eljentechnology.com/index.php/products/liquid-scintillators/71-e>) Saint Gobain BC-501 (<http://www.detectors.saint-gobain.com/uploadedFiles/SGdetectors/Documents/P>
- [7] <http://www.eljentechnology.com/index.php/products/paints/87-ej-520>.
- [8] <http://www.us.schott.com/borofloat/english/index.html> for details. Supplied by Glasteknik i Emmaboda AB, Utvägen 6 SE-361 31 Emmaboda, Sweden.
- [9] Poly-methyl-methacrylate, also known as PMM, acrylic, plexiglass, and lucite. Supplied by Nordic Plastics Group AB, Bronsyxegatan 6, SE-213 75 Malmö, Sweden.
- [10] <http://www.eljentechnology.com/index.php/products/paints/86-ej-510>.
- [11] <http://www.et-enterprises.com/files/file/Pmtbrochure11.pdf> for details.
- [12] H.H. Knox and T.G. Miller, *Nucl. Instrum. and Meth.* 101 (1972) 519, doi: 10.1016/0029-554X(72)90040-7.
- [13] J. Scherzinger et al., *Nucl. Instr. and Meth. in Phys. Res. A* 840 (2016) 121, doi:10.1016/j.nima.2016.10.011.

- [14] Scionix Holland BV. <http://www.scionix.nl>.
- [15] M. Moszyński et al., Nucl. Instr. and Meth. in Phys. Res. A 404 (1998) 157, doi:10.1016/S0168-9002(97)01115-7.
- [16] Hamamatsu Photonics. <http://www.hamamatsu.com>.
- [17] R. Billnert, S. Oberstedt, E. Andreotti, M. Hult, G. Marissens, A. Oberstedt, Nucl. Instr. and Meth. in Phys. Res. A 674 (2011) 94, doi:10.1016/j.nima.2011.05.034.
- [18] R. Brun and F. Rademakers, Nucl. Instr. and Meth. in Phys. Res. A 389 (1997) 81-86. See also <http://root.cern.ch/>.
- [19] A. Jhingan et al., Nucl. Instr. and Meth. in Phys. Res. A 585 (2008) 165, doi:10.1016/j.nima.2007.11.013.
- [20] A. Lavagno et al., Nucl. Instr. and Meth. in Phys. Res. A 617 (2010) 492, doi:10.1016/j.nima.2009.10.111.
- [21] I.A. Pawelczak et al., Nucl. Instr. and Meth. in Phys. Res. A 711 (2013) 21, doi:10.1016/j.nima.2013.01.028
- [22] A.G. Kozlov, B.A. Moiseenko, V.B. Pavlovich, E.G. Ponomarev, N.D. Tyufyakov, A.S. Shtan'ko, V.S. Yaskevich, A.G. Kovlov et al., translated from Atomnaya Énergiya 25 (1968) 534.